

Article

Investigating the Formation of Hot-Dry Rock in Gonghe Basin, Qinghai, China

Yang Yang¹, Fangbo Chen², Siliu Yu¹, Yubin Zheng¹, Sujie He¹, Yan Zeng¹, Xiaoli Xie^{1,*}, Jie Zhu^{3,*} and Nan Luo³

¹ School of Civil Engineering, Guangxi University of Construction, Nanning 530001, China

² CCB Housing Service Co., Ltd., Beijing 100005, China

³ Civil-Military Integration Center, China Geological Survey, Chengdu 610037, China

* Correspondence: xiaoli97531@163.com (X.X.); zjcugb0306@163.com (J.Z.)

Abstract: The Gonghe Basin, Qinghai Province, China, has rich geothermal and hot-dry rock resources. Through a magnetotelluric survey line with 400 points, combined with regional geology data, the deep geoelectrical structural background and thermal source mechanisms of the Gonghe Basin were explored. The results showed that (1) a deep structure with high conductivity may exist at a depth of 15 km in the basin, and could be compared to the layer-shaped, low-velocity, high-conductivity structure in the eastern part of the Qinghai–Tibet Plateau; (2) the rushing reverse fault played a crucial role in heat control and conduction from the hot field; and (3) high-temperature heat storage existed, including four layers of geothermal resources. This study proposed a triple-polymorphism model of hot-dry rock in the area; that is, the high-conductivity layer in the Middle–Late Cenozoic crust was the principal heat source; the Middle–Late Triassic granite was the essential heat-storing body, as well as a parent rock to the hot-dry rock; and the Cenozoic sedimentary rock was the effective caprock. This model is critical to understanding geothermal causes, predicting geothermal resources, and planning, on the Qinghai–Tibet Plateau.

Keywords: Gonghe Basin; hot-dry rock; heat source mechanism; magnetotelluric; geothermal energy



Citation: Yang, Y.; Chen, F.; Yu, S.; Zheng, Y.; He, S.; Zeng, Y.; Xie, X.; Zhu, J.; Luo, N. Investigating the Formation of Hot-Dry Rock in Gonghe Basin, Qinghai, China. *Minerals* **2023**, *13*, 1103. <https://doi.org/10.3390/min13081103>

Academic Editors: André Revil, Damien Jougnot and Jacques Deparis

Received: 29 June 2023

Revised: 17 August 2023

Accepted: 18 August 2023

Published: 19 August 2023



Copyright: © 2023 by the authors. Licensee MDPI, Basel, Switzerland. This article is an open access article distributed under the terms and conditions of the Creative Commons Attribution (CC BY) license (<https://creativecommons.org/licenses/by/4.0/>).

1. Introduction

Geothermal resources refer to geothermal energy, geothermal fluids, and their useful components on Earth that can be used economically by human beings. Geothermal resources can be divided into three types: shallow, hydrothermal, and hot-dry rock. Hot-dry rock resources refer to high-temperature rock masses with a general temperature higher than 180 °C, a depth of several kilometres, and no internal fluid, or only a small amount of underground fluid (dense and impermeable). In China, large-scale exploitable hot-dry rock resources have been discovered in the Gonghe Basin in Qinghai Province [1,2].

The Mediterranean–Himalayan belt of continental Eurasia is a major global hotspot for geothermal anomalies, with the Qinghai–Tibet Plateau being the most concentrated area of geothermal activity. Famous geothermal fields in the region include the Yangbajing–Yangyi, Kangding–Batang, Gonghe, and Guide Basins, with a heat flow of 300 mW/m². The Gonghe Basin is particularly rich in heat, with the temperature of the Qunaihai hot spring on the east side of the basin reaching 93–96 °C, surpassing the local boiling point [3]. In 2017, a dry thermal rock body with a temperature of 236 °C was discovered at depth in the Gongguki Basin, in the northeastern Qinghai–Tibet Plateau [4]). This discovery confirmed the richness of the geothermal resources of the Gonghe Basin, and has attracted the attention of local geothermal resource developers [5–7].

Several studies have been conducted to explain the formation of hot-dry rocks in the Gonghe Basin. Scholars believe that the radioactive decay of granite causes heat abnormalities in industrial areas [8]. Others believe that the Gonghe Basin is a typical conductive

thermal storage system, with heat originating deep within the basin, and transmitted to shallow parts through flower-shaped fractures throughout the basin [9–12]. Other researchers believe that the heat originates from the deep mantle [13]. All three arguments have a valid rationale, but they also have limitations, including uncertainty regarding the heat source mechanism, as well as the conduction and accumulation mechanisms. These arguments have hindered a full understanding of hot-dry rocks, the evaluation of geothermal resources, and the process of efficient development and utilisation.

This study focused on the Zhacang Thermal Field east of the Gonghe Basin, examining key elements, such as heat sources, water sources, heat storage, heat conduction, and accumulation processes from regional geology and geophysics, to investigate its possible heat mechanism, and establish a comprehensive genetic model to serve as a reference for the comprehensive evaluation of geothermal resources.

2. Geological Background

2.1. Regional Geology

The Gonghe Basin is located in the northeastern region of the Qinghai–Tibet Plateau [14,15]. Wakhong Mountain lies west of the basin, and is characterised by a slippery and broken terrain, and is adjacent to West Qinling Mountain. The eastern part of the basin is bordered by the Bayankra Basin with the Duomu Fault. On the southern side of the basin, the Anima–Qing Sewing Belt is adjacent to the Songpan–Ganzi Fold Belt, whereas the northern side of the basin is adjacent to the Qilian Mountains, south of Qinghai Lake (Figure 1).

The base of the Gonghe Basin formed during the Trinity Period, and was shaped during the middle and late stages of the Cretaceous Period [16–18]. Around the basin, the metamorphic sedimentary rocks formed by the East Kunlun and West Qinling Mountains are primarily sedimentary rocks, granite, and glittering long rocks that formed during the Trinity Period. The upper layers and hinterlands of the pots in the Gonghe Basin are dominated by new-generation sedimentary debris rocks that developed in the northwestern corner of the basin. A series of Cenozoic strata were deposited in the basin, and the overall trend in the west was thicker. The west side was approximately 6000 m thick, the Chabuzu Region in the central and eastern sections had a thickness of approximately 1500 m, and the Guide Area on the east side had a thickness of 500–1500 m.

There are more than 80 hot springs in the Gonghe Basin, with several key geothermal characteristics. Firstly, they are concentrated in the break zone. Secondly, they are primarily medium-temperature hot springs, with six springs having an outlet temperature exceeding 60 °C. The temperature of the Guide and Qunaihai hot springs on the east side of the basin are 96 °C and 97 °C, respectively, surpassing the local boiling point. In addition to the water thermal storage, which is dominated by shallow and new chips and ancient proxy crumbs, a deep dried hot rock was discovered in the area in 2017, within the Triassic granite, at a temperature of 236 °C [19].

2.2. Geophysical Characteristics of Hot-Dry Rock

The high-temperature hot-dry rock in the Gonghe Basin has the following physical features [20].

2.2.1. High Ground Temperature Field

According to Xue et al. [20], there are two magmatic rock belts on the western and eastern sides of the Gonghe Basin, striking nearly NNW. Based on the distribution of the magmatic rock belts, the study area can be divided into three parts: western, middle, and eastern (Figure 2).

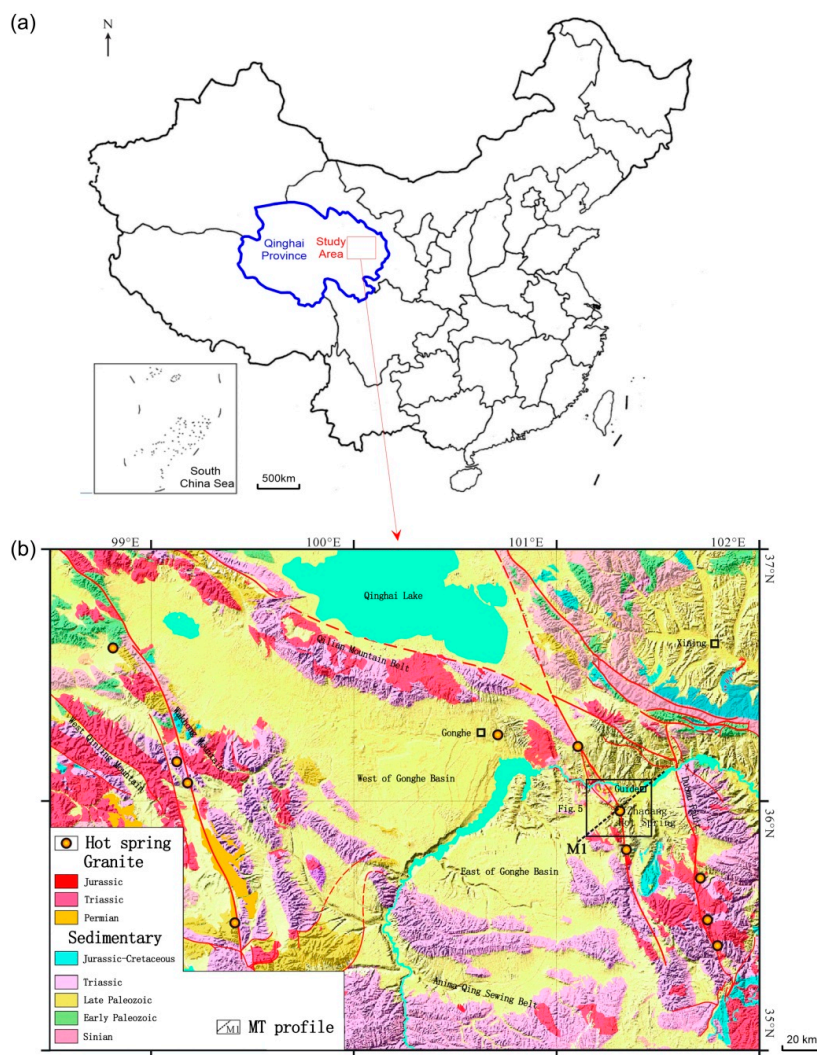


Figure 1. Map of the regional geology. (a) Location of the study area; (b) map of the regional geology in the Gonghe Basin. Profile M1 is the magnetotelluric (MT) survey line.

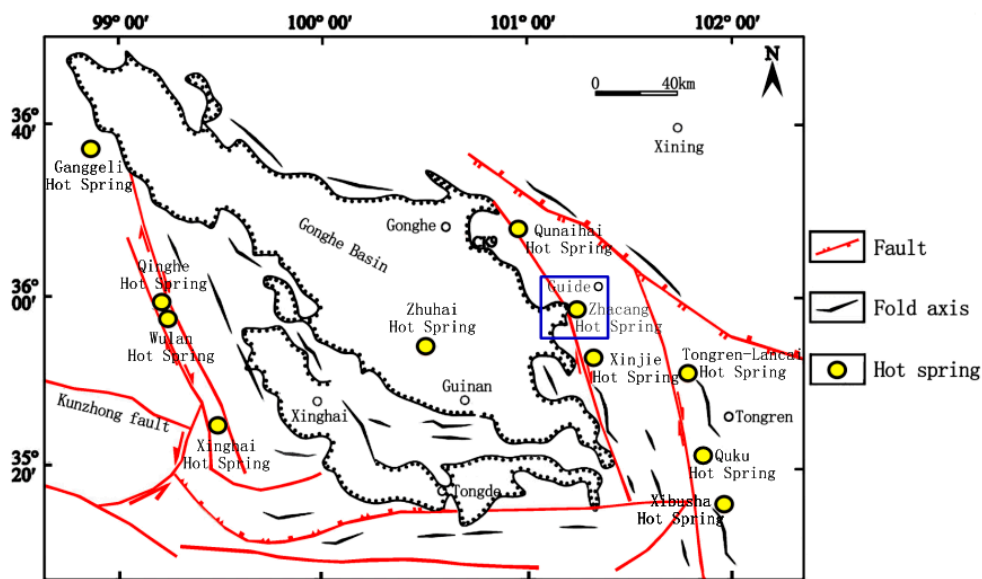


Figure 2. Geothermal distribution in the Gonghe Basin (cited from Xue et al. [20]). The blue box is the study area shown in Figure 5.

The magmatic rock belt on the west side of the basin is distributed on the front line of Wulan–Xinghai, along the Elashan Mountains, and stretches 180 km. The volcanic rock primarily strikes NNW, and exhibits a series of parallel fractures. Among them, Bhong Mountain breaks through the north and south, showing a strong squeezing phenomenon, and is characterised by a broken band 50 to 100 m wide, and multiple periods of activity [21].

The central Waligon Mountains, located in the middle of the basin, form a magmatic belt along the Maying Mountains. The Dangjia–Temple–Qunqiang hidden fracture belt runs NNW, along the Varigon Mountains to the north and south.

On the eastern side of the basin, a constructed magma belt lies along Zamhan Mountain, consisting of a three-layer system and Yanshan Period granite. Hot-spring distributions in this area include the Tongren–Lancai (67 °C) and Xibusha hot springs (44 °C).

2.2.2. Low Density and Weak Magnetism

According to Long et al. [22], a low-elevation gravity area formed in the Gonghe Basin (Figure 3).

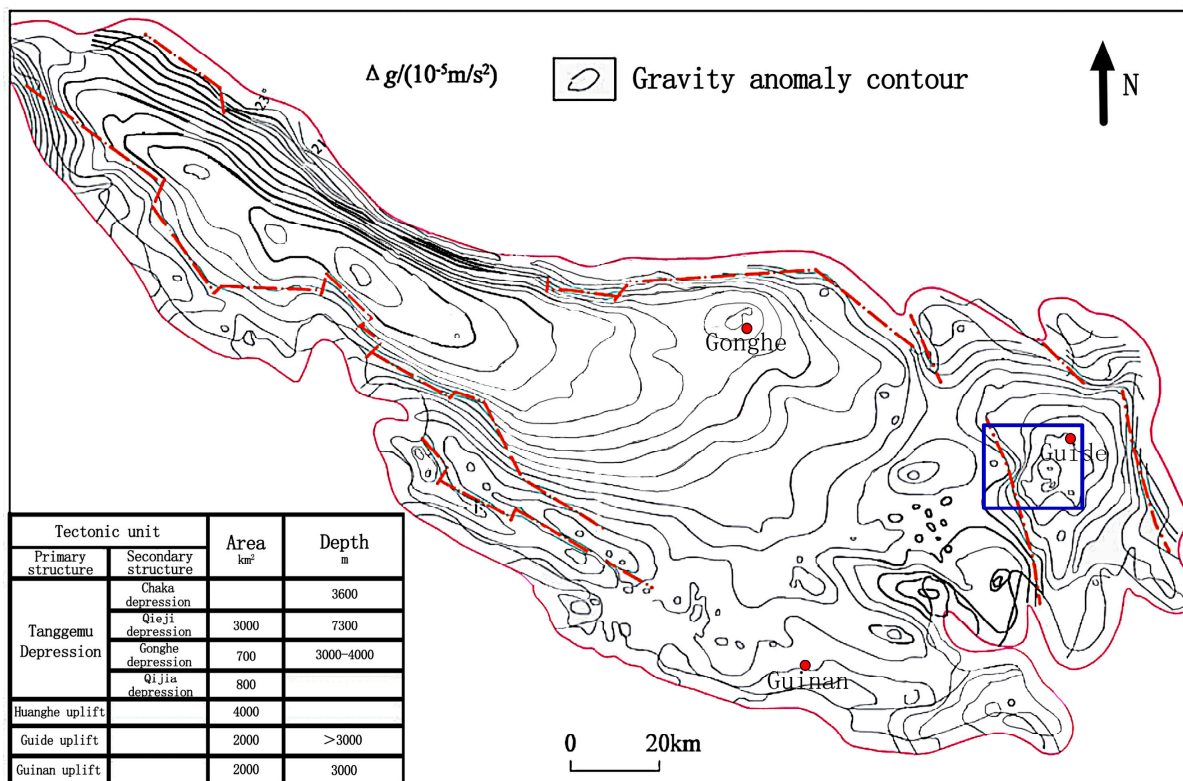


Figure 3. Gravity data of the Gonghe Basin (cited from Long et al. [22]). The blue box is the study area shown in Figure 5.

The aerial magnetic detection results indicate two NWW-band magnetic abnormalities in the study area: strong magnetic abnormalities in the north, caused by ancient cracks in the ultra-basic rock of Laji Mountain, with a range of 100–200 nT, and a low-to-middle magnetic abnormal belt along Gonghe, Guide, and other basins in the NWW. Based on the characteristics of the magnetic abnormality distribution, low magnetic abnormalities reflect a hidden magnetic body consistent with the Yanshan Period granite exposed north of Tongren. The granite zone consists of a series of weakly magnetic granites (Figure 4).

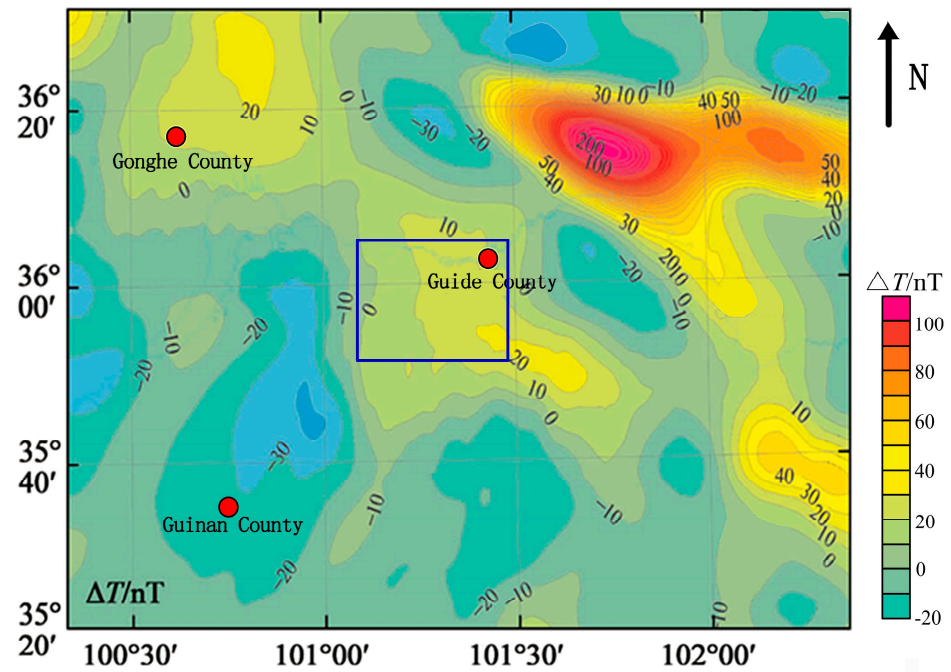


Figure 4. Airborne magnetic map of the Gonghe Basin (cited from Long et al. [22]). The blue box is the study area shown in Figure 5.

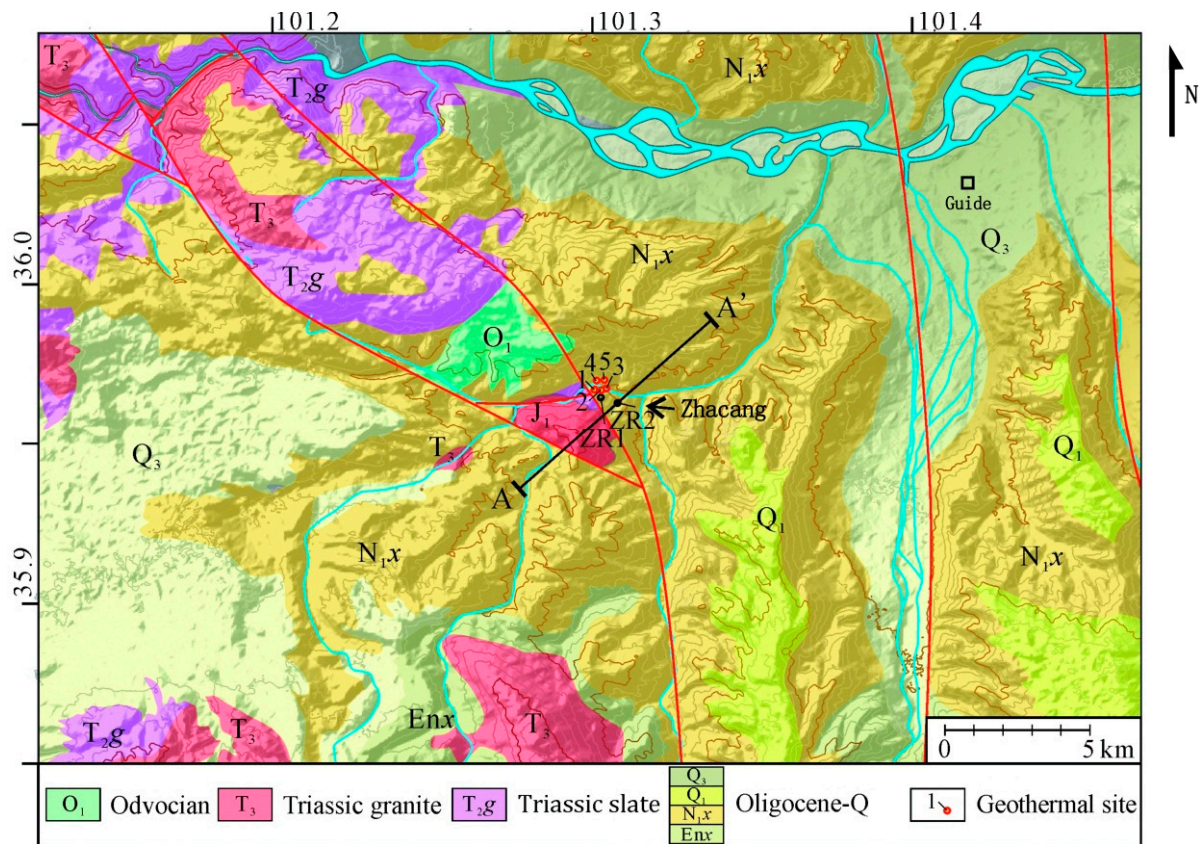


Figure 5. Geological diagram of the East Guide Zhacang geothermal field in the Gonghe Basin.

These geophysical characteristics indicate that the study area has a favourable foundation for the formation of hot-dry rocks.

2.3. Geothermal Geological Characteristics of the Zhacang Geothermal Field

The Zhacang geothermal field is situated on the eastern side of the Gonghe Basin, adjacent to the middle segment of the NNW-trending Varigon Fault (Figure 5; specific location is shown in Figure 1).

The fault is a strike-slip structure that runs NNW, and the occurrence of the outcrop section is at $206^{\circ} \angle 88^{\circ}$. Jurassic granite and granodiorite can be found at the foot of the outcrop of the geothermal field, covered by Early–Middle Triassic metasandstone (occurrence $82^{\circ} \angle 17^{\circ}$), and unconformably contacted by Neogene claystone. On the western side of the geothermal field, a secondary strike-slip fault, with a dip angle of $77\text{--}82^{\circ}$, has developed in the NW direction (Figure 6).

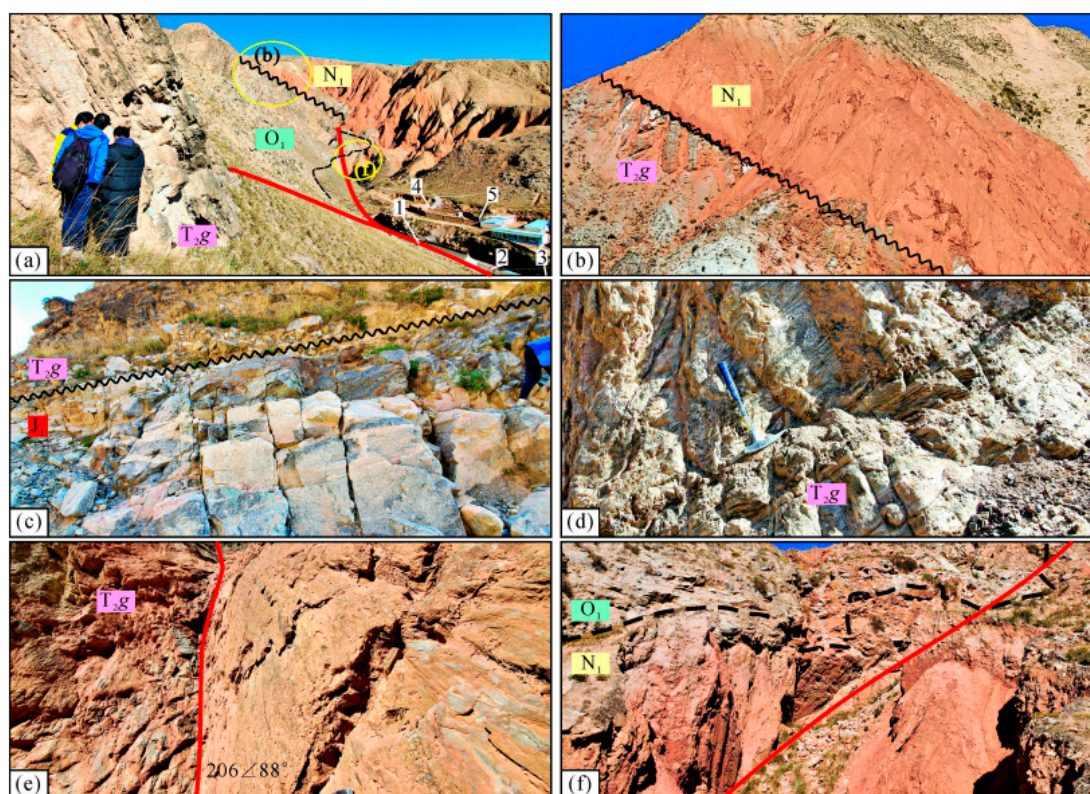


Figure 6. Typical field outcrop profile of the Zhacang geothermal field in the Gonghe Basin. (a) The NW-trending fault in a hot spring valley and geothermal drilling (1–5); (b) the unconformable contact between the Middle Triassic Gulang formation (T2g) and Neogene (N1); (c) the Middle Triassic Gulang formation metamorphic sand slate (T2g) and the underlying Jurassic granite (J1) have an unconformable contact relationship; (d) the field occurrence of metamorphic sand slate in the Middle Triassic Gulang formation; (e) the NW-trending fault steps and scratches indicate left-handed strike-slip features; (f) a normal fault developed in Neogene red clay rocks. The black curves in (a–c) represent the unconformity between strata.

The geothermal anomaly in the field is primarily concentrated in the Quaternary sandstone layer along the river valley, with temperatures ranging from 32 to 96°C , and a flow rate of $0.1\text{--}0.3$ L/s [23]). In addition, five local shallow boreholes revealed gas–liquid two-phase high-temperature fluids, with temperatures ranging from 93 to 96°C at depths of $90\text{--}100$ m, with an elevation of 2448 m, and a flow rate of 800 m³/d.

Since 2013, the Gonghe Basin has undergone several geothermal resource surveys, including those of the wells ZR1 and ZR2 (Figure 5), in the hot spring village of Guide Zhacang. These surveys confirmed the presence of deep wells in the eastern and western parts of the basin.

3. Methods

A total of 400 magnetotelluric (MT) survey points were collected in and around the Zhacang geothermal field (see Figure 1 for the location of profile M1), using a V8-6R/RXU-3E five-component instrument (Phoenix Geophysics). The data were collected using a “cross-shaped” five-component method, with a minimum observation time of 17 h per point, and a remote reference station was established 200 km from the measurement area. The effective frequency range of the observations was 320–0.0005 Hz, with 40 effective frequency points.

The data were then processed and inverted using MT-Pioneer software (V 5.1, developed by the Institute of Geology, China Earthquake Administration) and MT3DV software (V 2.0, developed by the Institute of Geology and Geophysics, Chinese Academy of Sciences). The MT-Pioneer software was used to preprocess the collected data first, achieving the preliminary processing of the collected MT data, such as the splicing of lines, correction of elevations, and removal of points with high noise. After the preprocessing, MT3DV software was used to invert the processed data, to realise the spatial inversion of the electric field data. In this study, because there was only one MT surveying line, 2D inversion was performed using the TM mode. Assuming that the resistivity ρ corresponded to the first high-frequency point, the total depth H was calculated as $H = 503 \sqrt{\frac{\rho}{f}}$. During the inversion, a uniform half-space was used as the initial model, and its resistivity was that corresponding with the last frequency point. In addition, a 0.5 km \times 0.5 km grid was used, the number of grids was 90 \times 50, and the search range of resistivity of each layer was from 0.1 to 1000 Ω ·m. For the objective function constructed by the relative error, the iteration stop condition was: root-mean-square (RMS) < 0.1.

4. Results

The MT measurements revealed three main electrical structural blocks in the Guide area (Figure 7).

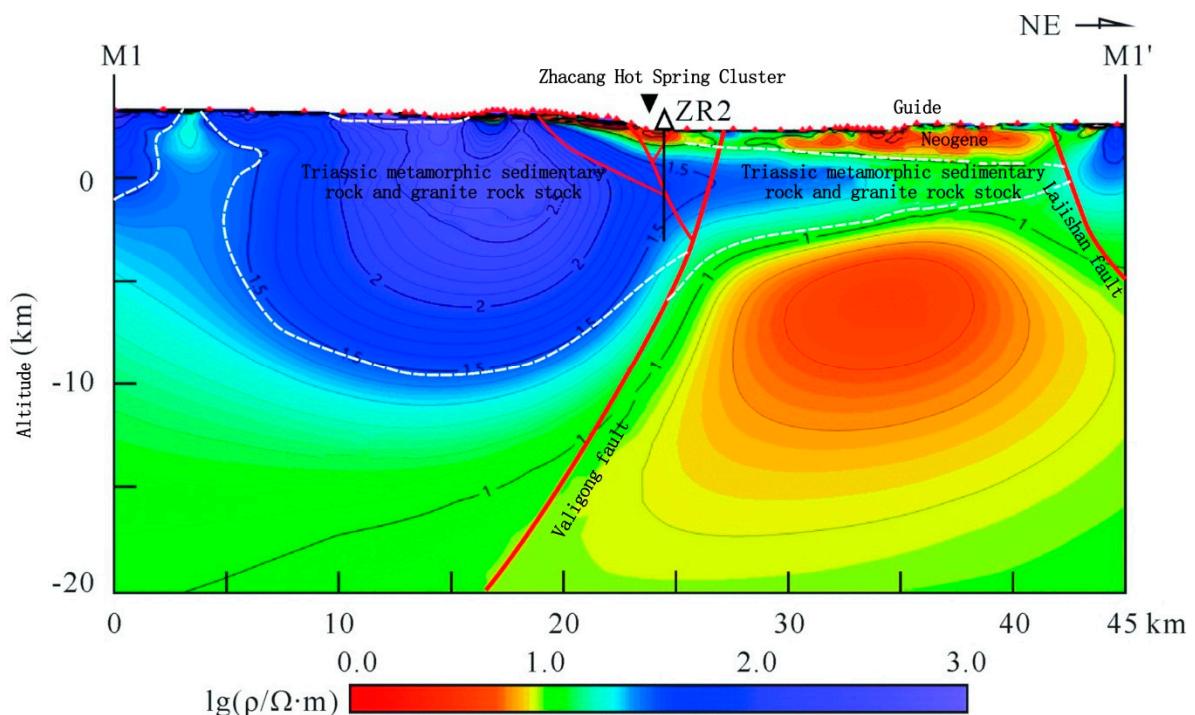


Figure 7. Resistivity profile of the MT line on the east side of the Gonghe Basin (see Figure 1 for the location of the M1 profile).

The first block is a low-resistivity surface layer, with a resistivity of less than 15 Ω ·m in the high-frequency band, at the shallow part on the right side of the survey line, reaching

depths of approximately 1.5 km. This block was inferred to represent Neogene strata in the basin area, primarily distributed east of the Varigon Fault.

The second block is a large-scale, high-resistivity body, with a resistivity of approximately 150–1000 $\Omega\cdot\text{m}$, primarily west of the Varigon Fault (on the left side of the survey line). This layer may be an abnormally high-resistivity granite body intruding into Triassic metamorphic sedimentary rocks, with a depth of approximately 20 km.

The third block is a large-scale, low-resistivity body of approximately 1–10 $\Omega\cdot\text{m}$, east of the Varigon Fault (on the right side of the survey line), which is approximately 20 km deep. Given that the water content of granite in the Gonghe Basin is approximately 0.9%, the characteristics of low resistivity and high conductivity may be related to its deep, high-temperature structure [24,25].

Several normal faults have developed along the survey line, and the Zhacang geothermal field is located in the Varigon Fault Zone, which has noticeable regional electrical features, and may have a large cutting depth and a steep slope.

With the use of the borehole data for well ZR2, a geological structural profile of the Zhacang geothermal field was prepared (Figure 8).

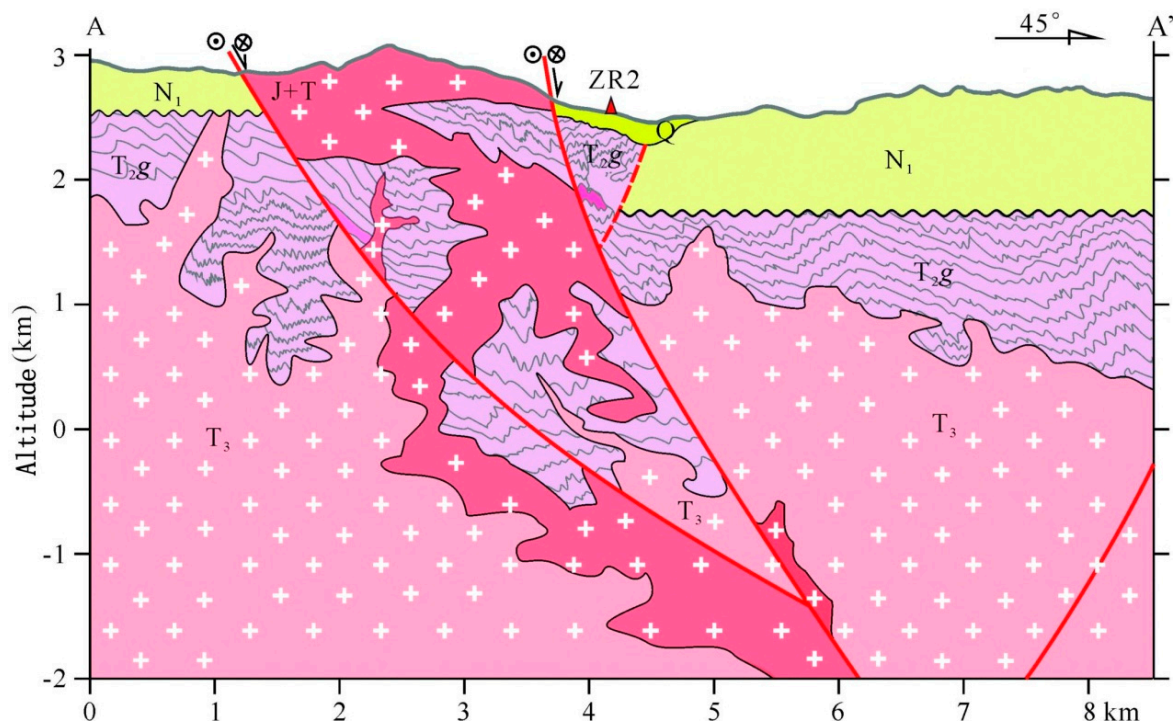


Figure 8. Geological structure of profile A–A' in the Zhacang geothermal field (see Figure 5 for the location of profile A–A').

5. Discussion

5.1. Heat Source Mechanism

Geothermal anomalies are abundant in the Gonghe Basin and its surroundings, and there is a long history of research on their heat sources. The three primary theories to explain the production of geothermal anomalies in the Gonghe Basin are the abnormal enrichment of radioactive elements in the crustal granite, mantle heat, and deep fracture heat conduction.

5.1.1. Radiogenic Heat Production Rate

The widespread development of granite is a notable feature of the Gonghe Basin. This granite is not only related to radiogenic heat, but also to the parent rock to the hot-dry rocks in the basin. Granite is rich in minerals containing uranium-series elements, and its radioactive energy generates and accumulates substantial heat energy, which may lead to

higher geothermal anomalies under suitable conditions [26,27]. Uranium-rich granites have been discovered in the coastal areas of southeastern China, with concentrations ranging from 6.28 to 7.56 $\mu\text{W}/\text{m}^3$ [28]. The Innamincka granite (320–300 Ma) in the Cooper Basin of Australia has a high radiogenic heat production rate (7–10 $\mu\text{W}/\text{m}^3$), which is considered the primary factor in the formation of the hot-dry Habanero rocks [29].

The Middle–Late-Triassic granites in the Gonghe Basin are primarily found in the central Qinling orogenic belt, which is a local manifestation of the regional tectonic–magmatic time covering the basin, and is considered a magmatic underplating event caused by lithospheric delamination [30]. Magmatic activity occurred at a time and location similar to those of the granites in the Songpan–Garze fold belt. Isotopic studies have shown that the magma is formed through the partial melting of crustal materials, and the source rocks are primarily argillaceous rocks or greywacke [31]. This study also found that the Middle Triassic metamorphic slate was highly deformed, and garnet, tourmaline, sillimanite, and other metamorphic minerals were formed locally. The granite that formed in the Gonghe Basin at 220–200 Ma may be related to a partial melting event during the detachment of the Songpan–Ganzi flysch fold belt, and crustal remelting was clearly induced by the detachment of the Triassic sedimentary basement, at a depth of 15 km [16,32,33].

Zhang [34] determined the radioactive heat generation rate of granite cores obtained from three geothermal boreholes in the Gonghe Basin to be $3.20 \pm 1.07 \mu\text{W}/\text{m}^3$. The heat flow contribution from the radioactive heat generation of granite, estimated via the thickened crust thickness, was approximately 30.4–40.5 mW/m^2 , accounting for approximately 29.6–39.7% of the average terrestrial heat flow in the Gonghe Basin. The global average radiogenic heat production rate of granites is 2.1–2.5 $\mu\text{W}/\text{m}^3$ [35,36], and the heat production rate is closely related to the age of the granite. Compared to typical geothermal fields dominated by radiogenic heat generation, the radiogenic heat generation rate of the granite in the Gonghe Basin is close to the global average value of Mesozoic–Cenozoic granite ($3.09 \pm 1.62 \mu\text{W}/\text{m}^3$), indicating that the magmatic granite does not show a strong anomaly in radiogenic heat production. Although the heat flow of radioactive elements contributes considerably, it is not the main heat source in magmatic basins. The cooling time of granites is typically 5–8 Ma, and granites from the Middle–Late Triassic in the Gonghe Basin have no residual heating capacity.

5.1.2. Low-Resistivity Layer in the Middle–Lower Crust as an Important Heat Source

The results of MT exploration indicate the presence of a low-resistivity block in the middle–lower crust of the Gonghe Basin (Figure 7; a resistivity less than 10 $\Omega\cdot\text{m}$). This layer may be an electrical reflection of a deep, high-temperature anomaly [37,38]. The low-resistivity layer is found 15–55 km beneath the basin, and is shallow in the north, and deep in the south. This layer also crosses the basin, including the Kunlun fault to the south, and is connected to the deep part of the Songpan fault, but may be blocked by the Qinling North fault zone at the north side, reducing its resistivity value; hence, it does not extend beyond the Haiyuan fault.

Bai [39] suggested that a low-resistivity layer, located between the Xianshuihe and Jinshajiang faults, developed 15 km below the crust in the eastern part of the Qinghai–Tibet Plateau, with a resistivity of less than tens of ohmmeters, and extended in a belt with a thickness of 20–30 km, indicating a ductile crustal flow in this area. Additionally, the position of the low-velocity layer, as interpreted via artificial seismic data, corresponds to this layer (velocity: approximately 5.8 km/s; thickness: approximately 8–10 km) [40–42], likely indicating the presence of a molten magma pocket 15 km underground. Tang [33] estimated the temperature at a depth of 15 km to be more than 650 °C, using the inversion of the S wave velocity and gravity data, and suggested that the ductile crustal flow in the middle–lower crust of eastern Tibet may be the primary heat source of the Litang–Batang geothermal anomaly.

Furthermore, based on gas isotope data from hot springs in the Gonghe Basin, the $^3\text{He}/^4\text{He}$ value is 0.04 to 0.08 Ra [43], indicating that the heat source for these springs is derived

from the crust, with no contribution from the mantle. Based on the regional geological background, geophysical data, hot spring occurrence, and gas isotope evidence, the ductile flow beneath the Songpan–Garze fold belt likely corresponds to the low-resistivity layer under the Gonghe Basin, which has similar geophysical characteristics, and may also be the main heat source for the Gonghe Basin.

5.2. Role of Granite in the Formation of Geothermal Resources in the Gonghe Basin

In this study, we determined the correlation between the dominant lithology and accumulation, and the dissipation of thermal energy in the basin. The results showed that the thermal conductivities of the granite, Triassic metamorphic sandstone slate, and overlying Oligocene claystone or siltstone were 2.79 ± 0.34 W/(m·K), 1.69 ± 0.31 W/(m·K), and 0.38 ± 0.10 W/(m·K), respectively. The granite has a relatively high thermal conductivity and diffusivity, with a thermal conductivity 1.69 times that of Triassic epimetamorphic rocks, and 7.5 times that of Cenozoic clastic rocks. This indicates that Triassic granite is more efficient in conducting or accumulating heat than the same heat source in other rocks under similar conditions, making it conducive to the formation of regional geothermal resources, such as hot-dry rocks. In contrast, the Cenozoic clastic rocks have poor heat conduction properties. However, a high thermal conductivity implies that granite areas have a relatively high capacity for heat dissipation under exposure conditions, whereas thick Cenozoic clastic sediments (5–8 km) likely form a regional cover that reduces heat dissipation and protects against heat accumulation in the granite.

5.3. Strike-Slip Fault Zone and Geothermal Anomaly

The Qinghai–Tibet Plateau has undergone a large-scale progressive uplift and deformation from south to north since the Cenozoic Era, accompanied by the compression of the Indian Plate towards the Eurasian Plate. In this context, the Gonghe Basin at the north-eastern margin of the plateau has developed NW–NNW-trending faults. These faults are characterised by a steep dip, a deep incision, and a sinistral strike-slip motion, influenced by the lateral extrusion mechanism. Geothermal anomalies in the basin, such as the hot springs in the Wahongshan fault zone in the west, the Qunaihai and Zhacang geothermal fields in the Varigon fault zone in the centre, and the Duohemao fault zone in the east and its surrounding areas, are characterised by rock formations or concentrated outcrops along the fault zone. The hot springs are concentrated in the fault zone, which could be due to two reasons: (1) the fault runs through the thermal reservoir, and acts as the main channel for pressure release and flow discharge; and (2) the fault zone cuts into the deep granite thermal reservoir with a high thermal conductivity, forming a local convective thermal reservoir channel.

Based on the electrical structure profile, the hot light fault (the middle branch of the Varigon fault) where the Zhacang geothermal field is located has a high resistivity anomaly (>100 $\Omega\cdot\text{m}$) on the left side of the granite development area, and a low resistivity anomaly on the right side of the fault, towards Laji Mountain. The electrical and stratigraphic development features are similar to those of the Nanshan fault zone in Qinghai. This indicates that the areas north and east of the NS strike-slip fault zone do not belong to the Gonghe Basin, based on their tectonic attributes. The Varigon strike-slip fault zone is an important structural and heat control boundary at the eastern side of the Gonghe Basin.

5.4. Formation Model

In this study, we proposed a ternary thermal accumulation model of hot-dry rocks in the Gonghe Basin (Figure 9), based on the deep geological structural characteristics of the regional geological and geophysical inversion data; the development law of surface geothermal anomalies; the formation and thermal reservoir structure revealed by drilling; the chemical, hydrogen, and oxygen isotope characteristics of water samples; and the thermal physical parameters of the rocks.

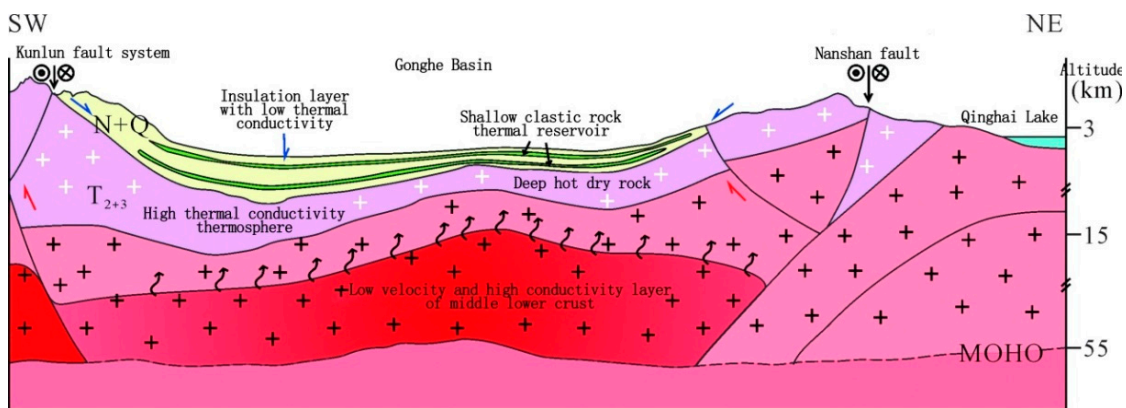


Figure 9. Accumulation pattern of deep geothermal energy in the Gonghe Basin.

The principal heat source is the high-temperature, low-velocity, and high-conductivity layer in the middle and lower Cenozoic crust, and the uplift of the crust to the middle and upper crusts caused by the simple shear of strike-slip faults produces abnormally high regional temperatures. Because of its high thermal conductivity and low water content, the Middle and Late Triassic granite is an essential heat conductor, as well as a hot-dry parent rock, and an important heat reservoir. The Cenozoic sedimentary rock, which has a low thermal conductivity, serves as an effective cover. Shallow surface water infiltrates and circulates near the granite body, forming a clastic-rock-type hydrothermal system, whereas deep granite forms a hot-dry rock system. The nearly-NNW-trending sinistral strike-slip fault zone cuts through a shallow thermal reservoir and deep granite body (hot-dry rock), and serves as an important heat-conducting and heat-controlling structure. Several areas affected by the N–E strike or nearly-E–W strike tensional normal faults that formed during the Cenozoic deformation of the northeastern margin of the Qinghai–Tibet Plateau may have played a key role in controlling the water flow. The pressure-relief areas formed at the intersection of these two groups of faults were favourable for the concentrated distribution of hot springs.

6. Conclusions

The following conclusions can be drawn from this study:

(1) The MT surveying revealed three electrical blocks in the Gonghe Basin. The first block was the overlying Cenozoic clastic sedimentary rock with a low resistivity (less than $15 \Omega \cdot m$), the second block was the Triassic granite with a high resistivity (approximately $150\text{--}1000 \Omega \cdot m$), and the third block was the Cenozoic middle–lower crust layer with a low resistivity (approximately $1\text{--}10 \Omega \cdot m$).

(2) The three blocks composed a three-component heat accumulation model for hot-dry rocks in the basin. The main heat source was the Cenozoic middle–lower crust layer with a high temperature, a low velocity, and a low resistivity (approximately $1\text{--}10 \Omega \cdot m$); the Triassic granite with a high resistivity (approximately $150\text{--}1000 \Omega \cdot m$) served as both the mother rock to hot-dry rocks, and a heat-storing body; the Cenozoic clastic sedimentary rock was a good caprock, with a low thermal conductivity and a low resistivity (less than $15 \Omega \cdot m$).

(3) The layered low-resistivity and high-conductivity anomalies in the Gonghe Basin at a depth of 15 km were correlated with the layered low-velocity and high-conductivity layers in the middle and lower crust during the deformation of the northeastern margin of the Qinghai–Tibet Plateau in the Cenozoic era. These layers may have been the main heat source for the hot-dry rocks and abundant hydrothermal geothermal anomalies in the basin.

(4) The NW–NS-trending strike-slip fault was a key heat-controlling and heat-conducting fault in the Zhacang geothermal field, and an important heat-controlling boundary in the eastern part of the Gonghe Basin.

(5) There are two types of geothermal resources in the four layers: medium–low temperature geothermal reservoirs in the shallow Cenozoic clastic rocks, and medium–high temperature geothermal reservoirs in the deep granite.

Author Contributions: Conceptualisation, Y.Y. and X.X.; methodology, F.C., Y.Z. (Yubin Zheng), and S.H.; software, S.Y.; validation, S.Y. and Y.Z. (Yubin Zheng); formal analysis, S.Y., Y.Z. (Yubin Zheng), and Y.Z. (Yan Zeng); writing—original draft preparation, Y.Y., X.X. and N.L.; writing—review and editing, Y.Y., Y.Z. (Yubin Zheng), Y.Z. (Yan Zeng), X.X. and J.Z.; supervision, J.Z. All authors have read and agreed to the published version of the manuscript.

Funding: This research was supported by the Basic Ability Improvement Project of Young and Middle-aged Teachers in Universities of Guangxi: Research on the Application of Construction Waste Concrete in Sound Insulation Mortar (No. 2022KY1166).

Data Availability Statement: The data that support the findings of this study are available from the corresponding author upon reasonable request.

Conflicts of Interest: The authors declare no conflict of interest.

References

1. Xu, T.; Hu, Z.; Li, S.; Jiang, Z.; Hou, Z.; Li, F.; Liang, X. Enhanced geothermal system: International progresses and research status of China. *Acta Geol. Sin.* **2018**, *92*, 1936–1947.
2. Mao, X.; Guo, D.; Luo, L.; Wang, T. The global development process of hot dry rock (enhanced geothermal system) and its geological background. *Geol. Rev.* **2019**, *65*, 1462–1472.
3. Zhang, C.; Jiang, G.; Shi, Y.; Wang, Z.; Wang, Y.; Li, S.; Jia, X.; Hu, S. Terrestrial heat flow and crustal thermal structure of the Gonghe–Guide area, northeastern Qinghai–Tibetan plateau. *Geothermics* **2018**, *72*, 182–192. [[CrossRef](#)]
4. Gao, J.; Zhang, H.; Zhang, S.; Chen, X.; Cheng, Z.; Jia, X.; Li, S.; Fu, L.; Gao, L.; Xin, H. Three-dimensional magnetotelluric imaging of the geothermal system beneath the Gonghe basin, Northeast Tibetan Plateau. *Geothermic* **2018**, *76*, 15–25. [[CrossRef](#)]
5. Anees, A.; Zhang, H.; Ashraf, U.; Wang, R.; Thanh, H.V.; Radwan, A.E.; Ullah, J.; Abbasi, G.R.; Iqbal, I.; Ali, N.; et al. Sand-ratio distribution in an unconventional tight sandstone reservoir of Hangjinqi area, Ordos Basin: Acoustic Impedance Inversion-Based Reservoir Quality Prediction. *Front. Earth Sci.* **2022**, *10*, 1018105. [[CrossRef](#)]
6. Thanh, H.V.; Zamanayad, A.; Safaei-Farouji, M.; Ashraf, U.; Hemeng, Z. Application of hybrid artificial intelligent models to predict deliverability of underground natural gas storage sites. *Renew. Energy* **2022**, *200*, 169–184. [[CrossRef](#)]
7. Rashid, M.; Luo, M.; Ashraf, U.; Hussain, W.; Ali, N.; Rahman, N.; Anees, A. Reservoir Quality Prediction of Gas-Bearing Carbonate Sediments in the Qadirpur Field: Insights from Advanced Machine Learning Approaches of SOM and Cluster Analysis. *Minerals* **2023**, *13*, 29. [[CrossRef](#)]
8. Zhang, C.; Jiang, G.; Jia, X.; Li, S.; Zhang, S.; Hu, D.; Hu, S.; Wang, Y. Parametric study of the production performance of an enhanced geothermal system: A case study at the Qiabugia geothermal area, northeast Tibetan plateau. *Renew. Energy* **2019**, *132*, 959–978. [[CrossRef](#)]
9. Yan, W.; Wang, Y.; Gao, X.; Zhang, S.; Ma, Y.; Shang, X.; Guo, S. Distribution and aggregation mechanism of geothermal energy in Gonghe basin. *Northwestern Geol.* **2013**, *46*, 223–230.
10. Zhang, S.; Yan, W.; Li, D.; Jia, X.; Zhang, S.; Li, S.; Fu, L.; Wu, H.; Zeng, Z.; Li, Z.; et al. Characteristics of geothermal geology of the Qiabuqia HDR in Gonghe basin, Qinghai Province. *Geol. China* **2018**, *45*, 1087–1102.
11. Yang, Y.; Wang, X.; Liang, M.; Jiang, Z.; Ou, Y.; Tang, X.; Li, X.; Qiu, L.; Liang, M.; Liu, D.; et al. Three-Dimensional Electromagnetic Imaging of Geothermal System in Gonghe Basin. *Minerals* **2023**, *13*, 883. [[CrossRef](#)]
12. Safaei-Farouji, M.; Thanh, H.V.; Dai, Z.; Mehbodniya, A.; Rahimi, M.; Ashraf, U.; Radwan, A.E. Exploring the power of machine learning to predict carbon dioxide trapping efficiency in saline aquifers for carbon geological storage project. *J. Clean. Prod.* **2022**, *372*, 133778. [[CrossRef](#)]
13. Feng, Y.; Zhang, X.; Zhang, B.; Liu, J.; Wang, Y.; Jia, D.; Hao, L.; Kong, Z. The geothermal formation mechanism in the Gonghe basin: Discussion and analysis from the geological background. *China Geol.* **2018**, *1*, 331–345. [[CrossRef](#)]
14. Zhang, G.; Guo, A.; Yao, A. Western Qinling Songpan continental tectonic node in China’s continental tectonics. *Earth Sci. Front.* **2004**, *11*, 23–32.
15. Zhang, K.; Zhang, Y.; Tang, X.; Xia, B. Late Mesozoic tectonic evolution and growth of the Tibetan plateau prior to the Indo-Asian collision. *Earth-Sci. Rev.* **2012**, *114*, 236–249. [[CrossRef](#)]
16. Zhang, K. Is the Songpan-Ganzi terrane (central China) really underlain by oceanic crust. *J. Geol. Soc. India* **2001**, *57*, 223–230.
17. Zhang, K. Escape hypothesis for the North and South China collision and the tectonic evolution of the Qinling orogen, eastern Asia. *Eclogae Geol. Helv.* **2002**, *95*, 237–247.
18. Zeng, L.; Zhang, K.; Tang, X.; Zhang, Y.; Li, Z. Mid-Permian rifting in central China: Record of geochronology, geochemistry and Sr-Nd-Hf isotopes of bimodal magmatism on NE Qinghai–Tibetan Plateau. *Gondwana Res.* **2018**, *57*, 77–89. [[CrossRef](#)]

19. Kong, L.; Li, D.; Zhang, S.; Luo, K. Preliminary study on hydrothermal sediment and hydrothermal alteration of Qunaihai hot spring in Guide Country, Qinghai Province. *J. Qinghai Univ.* **2019**, *37*, 83–89.
20. Xue, J.; Gan, B.; Li, B.; Wang, Z. Geological-geophysical Characteristics of Enhanced Geothermal Systems (Dry Hot Rocks) in Gonghe-guide Basin. *Geophys. Geochem. Explor.* **2013**, *37*, 35–41.
21. Yuan, D.; Zhang, P.; Liu, X. Late Quaternary tectonic activity of the Qinghai Elashan fault zone and the deformation mechanism of the northeastern margin of the Qinghai Tibet Plateau reflected by it. *Geosci. Front.* **2004**, *11*, 393–402.
22. Long, Z.; Xue, G.; Zhou, N.; Wu, Y.; Zhu, W. Investigation of deep geothermal resources in guide basin by using geophysical method. *Prog. Geophys.* **2009**, *24*, 2261–2266.
23. Jiang, Z.; Xu, T.; Owen, D.; Jia, X.; Feng, B.; Zhang, Y. Geothermal fluid circulation in the Guide basin of the northeastern Tibetan Plateau: Isotopic analysis and numerical modeling. *Geothermics* **2017**, *71*, 234–244. [[CrossRef](#)]
24. Chen, X.; Zhao, G.; Tang, J. The adaptive regularized inversion algorithm for magnetotelluric data. *Chin. J. Geophys.* **2005**, *48*, 1005–1016. [[CrossRef](#)]
25. Jiang, J.; Dai, L.; Li, H.; Shan, S.; Hu, H.; Hui, K. Influential factors and conduction mechanism of the in-situ electrical conductivity measurements of Earth's interior materials: A case study on crustal minerals. *Adv. Earth Sci.* **2013**, *28*, 455–466.
26. Li, X.; Sun, Z.; Zhou, W. *Paleo-Hydrothermal System and Uranium Mineralization*; Geological Publishing House: Beijing, China, 2000.
27. Wang, J. *Geothermal and Its Applications*; Science and Technology Publishing House: Beijing, China, 2015.
28. Lin, L.; Sun, Z.; Wang, A.; Liu, J.; Wan, J.; Li, X.; Luo, X. Radioactive geochemical characteristics of Mesozoic granites from Nanling region and southwest coastal region and their constraints on lithospheric thermal structure. *Acta Petrol. Mineral.* **2017**, *36*, 488–500.
29. Ayling, B.; Hogarth, R.; Rose, P. Tracer testing at the Habanero EGS site, central Australia. *Geothermics* **2016**, *63*, 15–26. [[CrossRef](#)]
30. Zhang, H.; Chen, Y.; Xu, W.; Liu, R.; Yuan, H.; Liu, X. Granitoids around Gonghe basin in Qinghai Province: Petrogenesis and tectonic implications. *Acta Petrol. Sin.* **2006**, *22*, 2910–2922.
31. Shi, Z.; Zhang, H.; Cai, H. Petrogenesis of strongly peraluminous granites in markan Area, Songpan Fold Belt and its tectonic implication. *Earth Sci. (J. China Univ. Geosci.)* **2009**, *34*, 569–584.
32. Reid, A.; Wilson, C.; Liu, S. Structural evidence for the Permo-Triassic tectonic evolution of the Yidun Arc, eastern Tibetan plateau. *J. Struct. Geol.* **2005**, *27*, 119–137. [[CrossRef](#)]
33. Tang, X.; Zhang, J.; Pang, Z.; Hu, S.; Tian, J.; Bao, S. The eastern Tibetan Plateau geothermal belt, western China: Geology, geophysics, genesis, and hydrothermal system. *Tectonophysics* **2017**, *717*, 433–448. [[CrossRef](#)]
34. Zhang, S.; Zhang, L.; Tian, C.; Cai, J.; Tang, B. Occurrence geological characteristics and development potential of hot dry rocks in Qinghai Gonghe basin. *J. Geomech.* **2019**, *25*, 501–508.
35. Vila, M.; Fernández, M.; Jiménez, M. Radiogenic heat production variability of some common lithological groups and its significance to lithospheric thermal modeling. *Tectonophysics* **2010**, *490*, 152–164. [[CrossRef](#)]
36. Artemieva, I.; Thybo, H.; Jakobsen, K. Heat production in granitic rocks: Global analysis based on a new data compilation GRANITE 2017. *Earth-Sci. Rev.* **2017**, *172*, 1–26. [[CrossRef](#)]
37. Zhao, L.; Zhan, Y.; Sun, X.; Hao, M.; Zhu, Y.; Chen, X.; Yang, H. The hidden seismogenic structure and dynamic environment of the 21 January Menyuan, Qinghai, Ms 6.4 earthquake derived from magnetotelluric imaging. *Chin. J. Geophys.* **2019**, *62*, 2088–2100.
38. Chave, A.D.; Jones, A.G. *The Magnetotelluric Method, Theory, and Practice*; Cambridge University Press: New York, NY, USA, 2012.
39. Bai, D.; Unsworth, M.; Meju, M.; Ma, X.; Teng, J.; Kong, X. Crustal deformation of the eastern Tibetan plateau revealed by magnetotelluric imaging. *Nat. Geosci.* **2010**, *3*, 358–362. [[CrossRef](#)]
40. Wang, C.; Chan, W.; Mooney, W. Three-dimensional velocity structural of crust and upper mantle in southwestern China and its tectonic implications. *J. Geophys. Res.* **2003**, *108*, 2442.
41. Huang, J.; Zhao, D.; Zheng, S. Seismic tomography of the Sichuan-Yunan active tectonic region. *Chin. J. Geophys.* **2001**, *44*, 127–135.
42. Sun, J. Crust and upper mantle electrical structure detection on the eastern margin of the Tibetan Plateau and its tectonic significance. *Sci. China (Ser. D)* **2003**, *33*, 173–180.
43. Tan, H.; Zhang, W.; Chen, J.; Jiang, S.; Kong, N. Isotope and geochemical study for geothermal assessment of the Xining basin of the northeastern Tibetan Plateau. *Geothermics* **2012**, *42*, 47–55. [[CrossRef](#)]

Disclaimer/Publisher's Note: The statements, opinions and data contained in all publications are solely those of the individual author(s) and contributor(s) and not of MDPI and/or the editor(s). MDPI and/or the editor(s) disclaim responsibility for any injury to people or property resulting from any ideas, methods, instructions or products referred to in the content.